

Anomalous magnetic behavior in pseudobinary compounds of CeFe_2

P. K. Khowash*

West Virginia University, Morgantown, West Virginia 26506

(Received 4 June 1990)

We explain the anomalous magnetic behavior in the pseudobinary compounds of cubic Laves-phase $\text{Ce}(\text{Fe},M)_2$ ($M=3d, 4d,$ and $5d$ transition-metal atoms) in terms of d - f hybridization. Calculated cerium and iron moments in CeFe_2 are found to be antiparallel such that $\mu_{\text{Ce}}/\mu_{\text{Fe}} = -0.37$, which is in excellent agreement with the recent experimental value of -0.3 . The calculated l -projected density of states is utilized to explain in detail the nature of the hybridization (d - d - f) responsible for various anomalies in these pseudobinary compounds.

The magnetic properties of intermetallic compounds, in particular, are interesting, since nonmagnetic elements when combined may form compounds which carry a finite magnetic moment. On the other hand, an inverse behavior may also occur in the sense that the metals that carry magnetic moments individually may lose all their magnetic behavior, thus forming a nonmagnetic compound or even a superconducting one like CeCo_2 .

In recent years, the electronic structure of Ce and its compounds¹⁻⁴ have continued to elude us. For a long time Ce in CeFe_2 was thought to be tetravalent with no magnetic moment at all, but a recent L_{III} x-ray photoemission study showed that Ce indeed carries a nonintegral magnetic moment. Although a member of the rare-earth group, it has many properties²⁻⁴ in common with systems involving uranium, namely, the specific heat, electrical resistivity, thermoelectric power, and Curie temperature. Again, the minimum lattice constants are located at CeCo_2 for $\text{Ce}M_2$ compounds with $M = \text{Fe}, \text{Co}, \text{Ni}$ just as in uranium compounds but in contrast to the trend of the corresponding systems with normal trivalent rare-earth ions, where the minimum is located at Ni. Very recent experimental investigations indicate that the addition of metal additives such as aluminum⁵ and cobalt² to CeFe_2 substituting the Fe site destabilizes its magnetic behavior and often a total loss of magnetism is observed. Similar magnetic behavior is also observed in pseudobinary compounds of CeFe_2 formed with additives like Ru, Os, and Ir (Refs. 2, 6, and 7) but no such instability appears when impurities like Mn, Ni, and Rh (Refs. 3 and 8) are added. It is therefore clear that the magnetic behavior of these cubic Laves-phase $\text{Ce}(\text{Fe}_{1-x},M_x)_2$ compounds (where M is usually a $3d, 4d,$ or $5d$ transition metal dopant) is strongly dependent on the nature of the impurity added. This instigates a detailed electronic structure calculation of above mentioned pseudobinary compounds in order to confirm the anomalous magnetic behavior conclusively from a theoretical point of view.

In this paper we present for the first time, calculations of charge, spin, and partial densities of states for pure CeFe_2 system and a number of its pseudobinary compounds formed with additives like Al, Mn, Co, Ni, Pd,

Rh, Ru, Re, Os, and Ir using a fully self-consistent discrete variational⁹⁻¹¹ method within the local density framework. We chose a cluster of 26 atoms consisting of two distinct pairs of iron and cerium atoms from the CeFe_2 intermetallic compound in the MgCu_2 structure¹² (see Fig. 1). This choice of cluster accounts quantitatively for the interaction between the additive when substituted at the iron site and the host atoms and at the same time minimizes the computational cost. The charges at various metal sites are calculated. Use of the various matrix elements are made to generate the densities of states. These densities of states are then analyzed in detail to understand the nature of hybridization that is thought to be responsible for various anomalies in the pseudobinary compounds of $\text{Ce}(\text{Fe}_{1-x},M_x)_2$.

In the discrete variational method,⁹⁻¹¹ the matrix elements of the effective Hamiltonian for the one-electron Schrödinger equation are computed as discrete sums, rather than integrals, thus avoiding separate multicenter

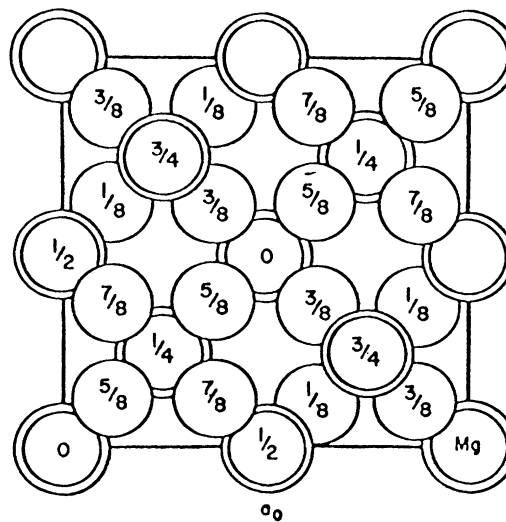


FIG. 1. The cubic MgCu_2 structure projected along a cubic axis.

integrals. The truly nonlocal Hartree-Fock exchange-correlation is approximated by the $X\alpha$ potential. The molecular-orbital eigenfunctions Ψ^α for the α th irreducible representation of the point group can be expanded in terms of a basis set of symmetry orbitals where the basis functions are chosen as a linear combination of atomic orbitals—molecular orbitals centered on different cluster atomic sites. The atomic potential binds only a limited number of states and therefore, to generate additional unoccupied states use of potential well with cutoff radius is made. These spherical potential wells reduce the overlap between orbitals of different atomic sites without affecting the diffuse conduction electron states significantly. The orbitals included in the valence region are $4f$, $5s$, $5p$, $5d$, $6s$, and $6p$ for Ce; $3d$, $4s$, and $4p$ for the $3d$ transition metals; $4d$, $5s$, $5p$ for Ru, Rh, and Pd and $5s$, $5p$, $5d$, $6s$, and $6p$ for $5d$ transition metal atoms, respectively. The discrete cluster energy levels obtained are then broadened with a Lorentzian of constant width to get a continuous density of states. The details of the method is given in the literature.^{9–11}

The pure CeM_2 system with M being Fe, Co, and Ni has been studied in details earlier using cluster¹³ (DV-LCAO) and band¹⁴ (linear muffin-tin orbitals) approaches. With use of the local-density theory we find a minimum in the lattice parameter for CeCo_2 in agreement with experiments. The electronic-structure calculations for pure CeFe_2 system gives an antiferromagnetic coupling of iron and cerium sites with magnetic moments of 1.42 and $1.99\mu\text{B}$ at the iron sites and -0.67 and $-0.62\mu\text{B}$, respectively, at the cerium atomic sites. Very recent powder neutron diffraction¹⁵ data identifies antiparallel coupling of cerium and iron moments such that $\mu_{\text{Ce}}/\mu_{\text{Fe}} = -0.3$ in excellent agreement with our calculated value of -0.37 . The average ionicities of Ce and Fe sites are close but not exactly equal and opposite due to the nonstoichiometric nature of the cluster chosen. The partial densities of states (see Ref. 13) indicate a strong hybridization of Fe $3d$ and Ce $4f$ states close to the Fermi energy which is responsible for the magnetic behavior of pure CeFe_2 .

Table I shows the Mulliken charge and spin distributions for pure CeFe_2 and for the different additives to

CeFe_2 substituted at the Fe site. It may be noted here that when other atomic species is introduced a local relaxation of the lattice around the impurity is expected which can reduce the symmetry of the material. This lack of symmetry makes computations difficult and expensive. Therefore in our calculations here, we have frozen the lattice at the experimental lattice constant as is true for most of the other state-of-the-art calculations and any lattice relaxation around the impurity is beyond the scope of this present work. This assumption, however, is expected not to change the general trend in our results. The bracketed numbers in Table I represent the net magnetization on the particular atomic species added to CeFe_2 . When the centrally located Fe is replaced by Co or Ni, we observe that the net magnetic moment on the additive reduces to $0.04\mu\text{B}$. The ionicity of neighboring and distant Ce increases a little while the iron site does not collect enough charge and thus becomes atomlike. Net magnetization on all the sites also decreases as compared to the pure host material. CeCo_2 and CeNi_2 are known to be paramagnetic^{13,14} in nature. The $3d$ states of Co and Ni [Figs. 2(a) and 2(b)] are pulled deeper in energy as compared to Fe due to their higher attractive central potential thereby reducing the degree of hybridization between $3d$ and $4f$ states. This diminishes the magnetic moment per formula unit of the defected material and confirms that increased concentration of Co and Ni additives push the system toward a paramagnetic phase.

In case of Mn-doped material, the ionicities of all the sites reduces a little as compared to the pure host but unlike Co and Ni, the impurity now retains its magnetic character with a magnetic moment of $1.07\mu\text{B}$. On the other hand, when Al is substituted at the Fe site in CeFe_2 , remarkable changes are seen. The ionicities of the next-nearest-neighbor iron atom shoots up with a considerable reduction of net magnetization on all the sites. The small moment at the Al site, arising from the extended $3p$ states, are now parallel to the Ce moments and this reduces the net magnetic moment per unit formula much faster while the iron moments continue to couple antiferromagnetically with that of Ce. This is in very good agreement with experiments³ where the magnetic susceptibility remains nearly the same for $\text{Ce}(\text{Fe}_x\text{Mn}_{1-x})_2$ but

TABLE I. Mulliken charge and spin distribution for pure CeFe_2 and for different additives to CeFe_2 . The bracketed numbers indicate the total spin on the particular atomic site. M denotes the additive indicated in the first column.

| | M | Ce | Fe | Ce |
|----|----------------|---------------|---------------|---------------|
| Fe | $-0.21(1.42)$ | $0.16(-0.67)$ | $-0.12(1.91)$ | $0.26(-0.62)$ |
| Co | $-0.26(0.04)$ | $0.21(-0.49)$ | $-0.07(1.29)$ | $0.34(-0.38)$ |
| Ni | $-0.29(0.04)$ | $0.26(-0.40)$ | $-0.03(1.33)$ | $0.40(-0.43)$ |
| Mn | $-0.18(1.07)$ | $0.12(-0.45)$ | $-0.17(1.20)$ | $0.22(-0.43)$ |
| Al | $-0.14(-0.02)$ | $0.20(-0.18)$ | $-0.49(1.07)$ | $0.26(-0.19)$ |
| Ru | $-0.37(0.03)$ | $0.34(-0.11)$ | $-0.21(0.99)$ | $0.44(-0.11)$ |
| Rh | $-0.60(0.42)$ | $0.60(-0.19)$ | $-0.03(1.85)$ | $0.73(-0.18)$ |
| Pd | $-0.82(0.17)$ | $0.70(-0.19)$ | $0.05(1.67)$ | $0.83(-0.16)$ |
| Re | $-0.27(-0.02)$ | $0.32(-0.13)$ | $-0.24(1.09)$ | $0.44(-0.13)$ |
| Os | $-0.41(0.10)$ | $0.42(-0.14)$ | $-0.04(0.97)$ | $0.55(-0.14)$ |
| Ir | $-0.55(0.04)$ | $0.56(-0.15)$ | $0.11(1.04)$ | $0.74(-0.11)$ |

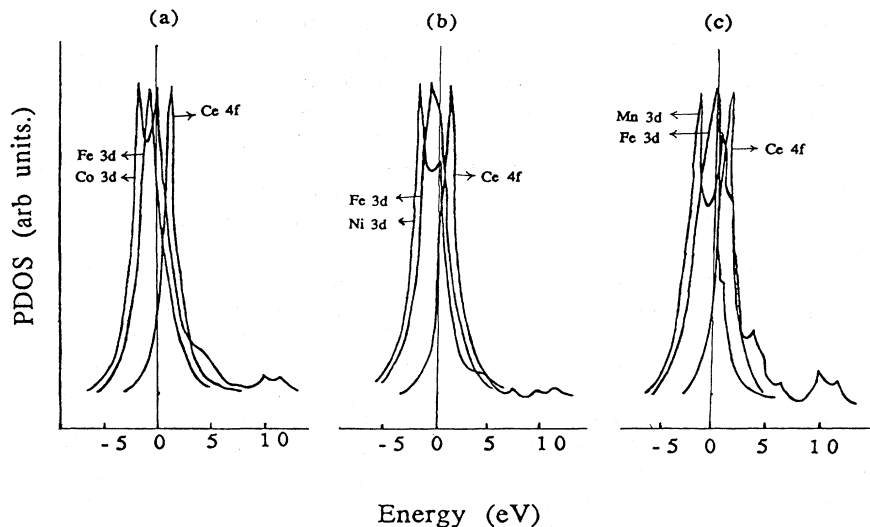


FIG. 2. Partial density of states for 3d transition metals substituted at the iron site in CeFe_2 . (a) Co 3d, Fe 3d, and Ce 4f in $\text{Ce}(\text{Fe}_x\text{Co}_{1-x})_2$, (b) Ni 3d, Fe 3d, and Ce 4f in $\text{Ce}(\text{Fe}_x\text{Ni}_{1-x})_2$, and (c) Mn 3d, Fe 3d, and Ce 4f in $\text{Ce}(\text{Fe}_x\text{Mn}_{1-x})_2$.

decreases sharply for $\text{Ce}(\text{Fe}_x\text{Al}_{1-x})_2$. The partial densities of states for $\text{Ce}(\text{Fe}_x\text{Mn}_{1-x})_2$ system is shown in Fig. 2(c). The wave function at -2.2 eV is composed of 43% Mn 3d, 6% Mn 4s, 10% Ce 6s, 5% Ce 5p, 3% Ce 4f, 1% Ce 5d, and 32% Fe 3d. The Mn 3d state hybridize strongly with Fe 3d states and Ce 4f states in the neighborhood of Fermi energy.

Among the 4d elements considered here, Ru behaves differently as compared to Rh or Pd. The charge accumulated on the Ru site is $0.37e$ with a net moment of $0.03\mu\text{B}$ whereas Ce gives away almost twice the charge as compared to pure host but with a drastic fall in their moments. The moment on the iron site which picks up a larger charge now is nearly halved. Rh and Pd added CeFe_2 , on the other hand, show small moment at the additive site as the 4d states gradually get filled. But the moment on the iron site does not change appreciably. These results are in excellent agreement with the susceptibility and resistivity measurements of Roy *et al.*¹⁶ where dramatic changes are reported for Ru added to CeFe_2 at the iron site but not for Rh or Pd. We now plot the l -projected densities of states in Fig. 3 to understand the nature of hybridization in Ru-, Rh-, and Pd-doped CeFe_2 . The peak at -2.2 eV [Fig. 3(a)] is due to 52% Ru 4d, 2% Ce 5p, 14% Ce 5d, 28% Fe 3d, 2% Fe 4s, and traces of Ce 4f. For Rh, the peak at -2.6 eV [Fig. 3(b)] is composed of 17% Rh 4d, 5% Ce 5d, 10% Fe 4s, 58% Fe 3d, 7% Ce 5d, and rest Ce 4f and 6p functions whereas in Fig. 3(c) (Pd-doped material), the wave function at -3.9 eV is solely from 58% Pd 4d, 5% Pd 5p, 3% Ce 5p, 4% Ce 5d, 12% Fe 4s, 1% Fe 4p, and 14% Fe 3d and 2% Ce 4f states. The Ce 4f states which was highly localized in the host system and for other 3d transition metal additives now takes a totally different form; a small peak just below the Fermi energy and larger peaks well above the Fermi energy in all the three cases. We also note that the degree of hybridization between Fe 3d states and additive 4d states decreases dramatically in going from Ru to Pd.

But the degree of hybridization of d - d - f states is much larger just below the Fermi level in case of Ru. The d states of Pd are nearly filled as the states are pulled down deeper inside the valence band as compared to Ru and Rh, due to its growing Z as discussed earlier for the case of 3d transition metal dopants, but now with pronounced intensity. The Fe 3d states are also pulled down in energy slightly. Again, the 3d bands of the additives plotted in Fig. 2 are much narrower than the 4d bands shown in Fig. 3. The Fe 3d and Ce 4f states continue to hybridize close to the Fermi energy but with much weaker intensity.

At this stage we decided to look into the effects of 5d transition metal additives like Re, Os, and Ir substituted at the iron site in CeFe_2 . The self-consistent charge distributions tabulated in Table I, show that the additives become active acceptors as in previous cases. The ionicities at all the sites increase gradually except for iron as we go from Re to Os to Ir; a situation similar to the case of 4d transition metal additives. The net magnetization at Re site is $-0.02\mu\text{B}$. This is due to the fact that the 5d state of Re with occupation 5.6 electrons generates a small moment of $0.01\mu\text{B}$ but the extended p functions produces a larger moment ($-0.03\mu\text{B}$) in the opposite sense leading to a net moment of $-0.02\mu\text{B}$. The nearest and the distant Ce sites show much smaller moments as compared to the host. The magnetization at the iron site is again lower than the host and is similar to the case of Al added material. It is therefore predicted that the 5d transition metal added CeFe_2 would grossly show similar magnetic behavior as in the case of $\text{Ce}(\text{Fe}_x\text{Al}_{1-x})_2$.

To summarize, we for the first time performed theoretical calculations to confirm that the pseudobinary compounds of CeFe_2 formed with 3d, 4d, and 5d transition metal atoms substituted at the Fe site show anomalous magnetic behavior. The electronic structure calculations for pure CeFe_2 show an antiferromagnetic coupling of Ce and Fe moments with $\mu_{\text{Ce}}/\mu_{\text{Fe}} = -0.37$ in excellent

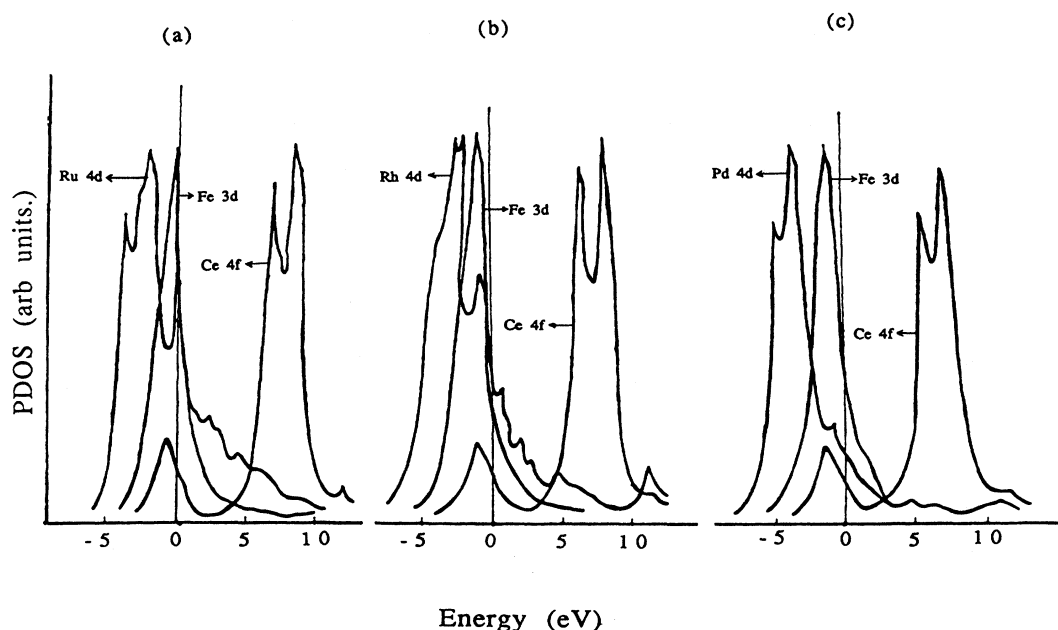


FIG. 3. Partial density of states for $4d$ transition metals substituted at the iron site in CeFe_2 . (a) Ru $4d$, Fe $3d$, and Ce $4f$ in $\text{Ce}(\text{Fe}_x\text{Ru}_{1-x})_2$, (b) Rh $4d$, Fe $3d$, and Ce $4f$ in $\text{Ce}(\text{Fe}_x\text{Rh}_{1-x})_2$ and (c) Pd $4d$, Fe $3d$, and Ce $4f$ in $\text{Ce}(\text{Fe}_x\text{Pd}_{1-x})_2$.

agreement with very recent powder neutron diffraction measurements ($\mu_{\text{Ce}}/\mu_{\text{Fe}} = -0.3$). For Co- and Ni-doped material the magnetization falls off gradually thereby pushing the system slowly toward a paramagnetic phase. However, not as much a dramatic change in magnetization is found for Mn, Rh, or Pd added systems as is observed for Al, Ru, Re, Os, and Ir additives. This is in excellent agreement with the recent magnetic susceptibility and electrical resistivity measurements. The Ce $4f$ states show very different structure for $3d$ and $4d$ transition metal additives producing very different degrees of $d-f$

hybridization. Again in the later case, the $d-d-f$ hybridization diminishes sharply in going from Ru to Pd. We believe that the anomalous magnetic behavior in the above-mentioned "pseudobinary" compounds are explained in terms of $d-d-f$ hybridization—thus resolving the problem.

ACKNOWLEDGMENTS

Helpful discussions with Dr. S. B. Roy are gratefully acknowledged.

*Permanent address: AT&T Bell Labs, Middletown, NJ 07748.

¹M. Croft, R. Neifield, B. Qi, G. Liang, I. Perez, S. Gunapala, F. Lu, S. Shaheen, E. G. Spencer, N. Stoffel, and M. denBoer, in *Proceedings of the Fifth International Conference on Valence Fluctuations* (Bangalore) 1986, edited by S. K. Malik and L. C. Gupta (Plenum, New York, 1987).

²A. K. Rastogi and A. P. Murani, in *Proceedings of the Fifth International Conference on Valence Fluctuations* (Ref. 1).

³D. F. Franceschini and S. F. da Cunha, *J. Magn. Mater.* **52**, 280 (1985).

⁴S. J. Kennedy, A. P. Murani, J. K. Cockcroft, S. B. Roy, and B. R. Coles, *J. Phys. Condens. Matter* **1**, 629 (1989).

⁵S. B. Roy and B. R. Coles, *J. Phys. Condens. Matter* **1**, 419 (1989).

⁶S. B. Roy and B. R. Coles, *J. Phys. F* **17**, L215 (1987).

⁷P. N. Tandon, P. G. Pillary, A. K. Grover, and V. Balasu-

bramanian (unpublished).

⁸S. B. Roy, S. J. Kennedy, and B. R. Coles, *J. Phys. (Paris)* **49**, 271 (1988).

⁹D. E. Ellis and G. S. Painter, *Phys. Rev. B* **2**, 2887 (1970).

¹⁰E. J. Baerends, D. E. Ellis, and P. Ros, *Chem. Phys.* **2**, 41 (1973).

¹¹P. K. Khowash and D. E. Ellis, *Phys. Rev. B* **36**, 3394 (1987).

¹²R. W. G. Wyckoff, *Crystal Structures* (Interscience, New York, 1963), Vol. 1, p. 365.

¹³P. K. Khowash, *Physica* (to be published).

¹⁴O. Erikson, L. Nordström, M. S. S. Brooks, and B. Johansson, *Phys. Rev. Lett.* **60**, 2523 (1988).

¹⁵S. J. Kennedy and B. R. Coles, *J. Phys. Condens. Matter* **2**, 1213 (1990).

¹⁶S. B. Roy and B. R. Coles, *Phys. Rev. B* **39**, 9360 (1989).